



(٣٦٣) - (٣٨٩)

العدد السابع

عشر

تأثير إجهاد الثنائي مع حالة الانزلاق مع الدوران على التدفق التمعجي لسائل باول آرينغ مع

تأثير قناة غير متماثلة مائلة مع وسط مسامي

رنا غازي إبراهيم ، لقاء زكي حمادي

جامعة بغداد/ كلية العلوم

liqqa.hummady@sc.uobaghdad.edu.iq

rana.ghazi1103a@cs.uobaghdad.edu.iq.

المستخلص:

في هذه المقالة ، تم فحص تأثير إجهاد الثنائي والشرط الانزلاقي ومتغير الدوران والمتغيرات الأخرى على التدفق التمعجي لسائل باول آرينغ في قناة غير متماثلة مائلة مع مجال مغناطيسي مائل عبر وسط مسامي مع نقل الحرارة . تم استخدام المعادلات التأسيسية التي تخضع لنموذج السائل باول آرينغ. تم استخدام افتراضات تقريب طول الموجة الطويلة وانخفاض عدد رينولدز في تحليل التدفق. تم ابتكار تعبيرات شكل مغلقة لدالة التدفق والكفاءة الميكانيكية. يتم التعبير عن توزيعات درجة الحرارة وتدرجات الضغط والسرعة المحورية رياضياً. من خلال جمع الأرقام ، تم شرح تأثير المعايير المختلفة وتمثيلها بيانياً. تم الحصول على هذه النتائج العديدة باستخدام التطبيق الرياضي

MATHEMATICA

للعلوم التربوية والنفسية وطرائق التدريس للعلوم الأساسية

الكلمات المفتاحية: إجهاد الثنائي ، انتقال الحرارة ، مجال مغناطيسي .

Effect of Couple-stress with Slip Condition and Rotation on Peristaltic Flow of a Powell-Eyring Fluid with the Influence of an Inclined Asymmetric Channel with Porous Medium

Rana Ghazi Ibraheem ، Liqaa Zeki Hummady

University of Baghdad / College of Science

rana.ghazi1103a@cs.uobaghdad.edu.iq. , liqqa.hummady@sc.uobaghdad.edu.iq.



Abstract

In this article, the effect of the couple-stress , slip condition, and the rotation variable and other variables on the peristaltic flow of Powell-Eyring fluid in an inclined asymmetric channel with an inclining magnetic field through a porous medium with heat transfer is examined. Constitutive equations obeying the Powell-Eyring fluid model are employed. Assumptions of long wave length approximation and low Reynolds number are used in flow analysis. The stream function and mechanical efficiency have closed form expressions devised. Distributions of temperature, pressure gradients, and axial velocity are expressed mathematically. Through the collection of figures, the impact of various criteria is explained and graphically represented. These numerical results were attained using the mathematical application MATHEMATICA.

Keywords: Couple stress, Heat transfer, Magnetic field .

1. Introduction

Peristaltic pumping is a particular type of pumping that occurs when a variety of complex rheological fluids may be easily transferred between two locations. The term "peristaltic" refers to this method of pumping. The ducts through which the fluid passes undergo intermittent involuntary constriction and then expand. As a result, the pressure gradient rises, causing the fluid to move forward. After Latham's groundbreaking work (Latham, 1966) and due to the fact that it is utilized in biological, engineering, and physiological systems academics have become increasingly interested in the different applications of peristalsis. Due to the fact that it is utilized in biological, engineering, and physiological systems, peristaltic transport has received significant attention in recent years. Generally, the peristaltic wave's circular contractions and the successive longitudinal contractions that occur during peristalsis are generated by the sinuses which propagate along the fluid-containing duct. This technique is the basis for several muscular tubes, including the gastrointestinal tract, fallopian tubes, bile ducts, ureters, esophageal tubes, and others. Moreover, non-Newtonian fluids are better than numerous industrial and physiological processes that use Newtonian



fluids. Among the models of non-Newtonian fluids (which can exhibit various rheological effects), that can be accessed is Paul-Earing fluid. Although this model is more difficult mathematically than models of non-Newtonian fluids, it deserves more attention because of its distinct benefits. Numerous researchers have been interested in the Powell-Eyring fluid's peristaltic flow mechanism since it was studied by Hina and Mustafa and Hayat and Alsaedi(Hina et al., 2016), Hayat and Naseema and Rafiq and Fua(Hayat et al., 2017), Hayat and Ahmed (Ali & Abdulhadi, 2018), Hussain and Alvi and Latif and Asghar(Hussain et al., 2019), and Ali and Liqaa(Hummady, 2022). The static magnetohydrodynamic flow and heat transfer of an Eyring-Powell fluid on an expansion plate with viscous dissipation were studied and numerically explained (Satya Narayana et al., 2017). The exchange of thermal energy between different system components is referred to as heat transfer. However, the medium's physical characteristics and the separate compartments' temperatures affect the speed. In recent years, research (Eldabe et al., 2020),(Noreen et al., 2020),(Khudair & Dwail, 2021),(Al-Khafajy, 2021) has been conducted about studying the effect of heat transport on non-Newtonian fluids. In a tapered asymmetric channel, the issue of peristaltic transport of an incompressible non-Newtonian fluid is examined(Ahmed, 2018). Peristalsis is used as the basis for the creation of devices such as peristaltic pumps, roller pumps, hose pumps, tube pumps, finger pumps, heart-lung machines, blood pump machines, and dialysis machines. These applications include the transportation of aggressive chemicals, high solid slurries, toxic (nuclear industries), and other materials. With regard to well-established problems of the stir of semi-conductive physiological fluids, such as blood and blood pump machines, magnetic drug forcing, and pertinent methods of human digestion, the advantage of applied magnetic field (MHD) on peristaltic efficacy is crucial. It is also helpful in treating gastroparesis, chronic constipation, and morbid obesity as well as magnetic resonance imaging (MRI), which is used to identify brain, vascular diseases, and tumors. A substance that has several tiny holes scattered throughout it is referred to as a porous medium. In riverbeds, fluid infiltration and seepage are sustained by



flows over porous media. Important examples of flows through a porous material are those through the ground, water, and oil. Oil is trapped in rock formations like limestone and sandstone, which make up the majority of an oil reservoir (Jasim, 2022). Natural porous media can be found in many different forms, such as sand, rye bread, wood, filters, bread loaves, human lungs, and the gallbladder. Food processing, oxygenation, hemodialysis, tissue condition, heat convection for blood flow from tissues' pores, and radiation between the environment and its surface all depend on the action of heat transfer in the peristaltic repositioning of fluid (Ali, 2022), (Aziz et al., 2021), (Kareem & Abdulhadi, 2020), (Hage & Hummady, 2022). The aforementioned processes all benefit from mass transfer; in particular, the mass transfer that occurs as nutrients diffuse from the blood into nearby tissues cannot be understated. Greater mass transfer participation is typical in the distillation, diffusion of chemical contaminants, membrane separation, and combustion processes. It should be observed that when mass and heat transmission happen at the same time, there is a connection between driving potentials and fluxes. However, the temperature gradient is what causes the gradients in mass flux and composition (termed Soret action). The study of fluid peristaltic transport in the presence of an external magnetic field and rotation is necessary for many issues involving the flow of conductive physiological fluids, such as blood and saline water (Mohaisen & Abdulhadi, 2022). A variety of values are used for the rotational parameters, the porous medium, density, amplitude wave, and taper of the channel, as well as a variety of values for the Hartman number and Darcy number, to study the effects of varying the velocity and pressure gradient. The ability to characterize rheologically complicated fluids like liquid crystals and human blood makes the study of pair stress fluid extremely helpful in understanding a variety of physical issues. Couple stress fluid refers to a specific type of non-Newtonian fluid in which the size of the fluid's particles is taken into consideration. Recent researches on the couple stress fluid has been conducted (Abdulhussein & Abdulhadi, 2022; Gamachu & Ibrahim, 2023; Prasad et al., 2023; Salman & Abdulhadi, 2018). The purpose of this study is to investigate the couple-stress, slip condition, and



rotation impacts of Powell-Eyring fluid peristaltic transport in porous media under the combined influence of inclined MHD.

2. Problem Mathematical description

Consider the peristaltic motion of an incompressible Powell-Eyring fluid in a two-dimensional, asymmetric conduit with a width of $(d'+d)$. An endless sinusoidal wave traveling along the channel walls at a constant forward speed (c) is what generates flow.

The geometry of the wall structure is described as:

$$\bar{h}_1(\bar{x}, \bar{t}) = d - a_1 \sin \left[\frac{2\pi}{\lambda} (\bar{X} - c\bar{t}) \right] \quad 1$$

$$\bar{h}_2(\bar{x}, \bar{t}) = -d' - a_2 \sin \left[\frac{2\pi}{\lambda} (\bar{X} - c\bar{t}) + \Phi \right] \quad 2$$

In which $\bar{h}_1(\bar{x}, \bar{t})$, $\bar{h}_2(\bar{x}, \bar{t})$ are the lower and upper walls respectively, (d, d') denote the channel width, (a_1, a_2) are the amplitudes of the wave, (λ) is the wavelength, (c) is wave the wave speed, (Φ) varies in the range $(0 \leq \Phi \leq \pi)$, when $\Phi = 0$ is a symmetric channel with out-of-phase waves and $\Phi = \pi$ waves are in phase, the rectangular coordinate system is chosen so that the $\bar{X} - axis$ is in the direction of the wave's motion. and the $\bar{Y} - axis$ perpendicular to \bar{X} , where \bar{t} is the time as shown in خطأ! لم يتم العثور على مصدر المرجع.

Further a_1, a_2, d, d' and Φ fulfill the following condition;

$$a_1^2 + a_2^2 + 2a_1a_2 \cos \Phi \leq (d + d')^2 \quad 3$$

The Cauchy stress tensor $\bar{\tau}$ for a fluid that obeys the Powell- Eyring model is given as follows:-

$$\bar{\tau} = -PI + \bar{S} \quad 4$$

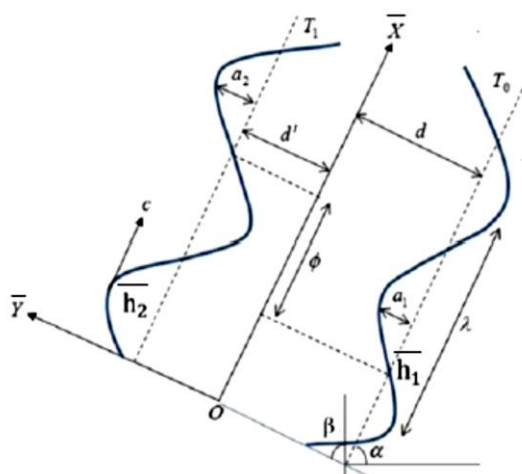


Figure 1: Coordinates for Inclined Asymmetric Channels in Cartesian Space

$$\bar{S} = \left[\mu + \frac{1}{\beta \dot{\gamma}} \sinh^{-1} \left(\frac{\dot{\gamma}}{c_1} \right) \right] A_{11} \quad 5$$

$$\dot{\gamma} = \sqrt{\frac{1}{2} \text{tr}(A_{11})^2} \quad 6$$

$$A_{11} = \nabla \bar{V} + (\nabla \bar{V})^T \quad 7$$

Where \bar{S} is the extra stress tensor, I is the identity tensor, $\nabla = (\partial \bar{X}, \partial \bar{Y}, 0)$ is the gradient vector, (β, c_1) are the material parameters of Powell-Eyring fluid, P is the fluid pressure, and μ the dynamic viscosity. The term \sinh^{-1} is approximately equivalent to

$$\sinh^{-1} \left(\frac{\dot{\gamma}}{c_1} \right) = \frac{\dot{\gamma}}{c_1} - \frac{\dot{\gamma}^3}{6c_1^3} \quad , \quad \left| \frac{\dot{\gamma}^5}{6c_1^5} \right| \ll 1 \quad 8$$

The flow is governed by three coupled nonlinear partial differentials of continuity, momentum, and energy, which are expressed in frame (\bar{X}, \bar{Y}) as



$$\frac{\partial \bar{U}}{\partial \bar{X}} + \frac{\partial \bar{V}}{\partial \bar{Y}} = 0 \quad 9$$

$$\begin{aligned} \rho \left(\frac{\partial \bar{U}}{\partial \bar{t}} + \bar{U} \frac{\partial \bar{U}}{\partial \bar{X}} + \bar{V} \frac{\partial \bar{U}}{\partial \bar{Y}} \right) - \rho \Omega \left(\Omega \bar{U} + 2 \frac{\partial \bar{V}}{\partial \bar{t}} \right) = - \frac{\partial \bar{P}}{\partial \bar{X}} + \frac{\partial \bar{S}_{\bar{X}\bar{X}}}{\partial \bar{X}} + \frac{\partial \bar{S}_{\bar{X}\bar{Y}}}{\partial \bar{Y}} - \\ \sigma \beta_0^2 \cos \beta (\bar{U} \cos \beta - \bar{V} \sin \beta) \\ - \frac{\mu}{k} \bar{U} - \mu_1 \nabla^4 \bar{U} + p g \sin \alpha^* \end{aligned} \quad 10$$

$$\begin{aligned} \rho \left(\frac{\partial \bar{V}}{\partial \bar{t}} + \bar{U} \frac{\partial \bar{V}}{\partial \bar{X}} + \bar{V} \frac{\partial \bar{V}}{\partial \bar{Y}} \right) - \rho \Omega \left(\Omega \bar{V} + 2 \frac{\partial \bar{U}}{\partial \bar{t}} \right) = \\ - \frac{\partial \bar{P}}{\partial \bar{Y}} + \frac{\partial \bar{S}_{\bar{X}\bar{Y}}}{\partial \bar{X}} + \frac{\partial \bar{S}_{\bar{Y}\bar{Y}}}{\partial \bar{Y}} - \sigma \beta_0^2 \sin \beta (\bar{U} \cos \beta - \bar{V} \sin \beta) \\ - \frac{\mu}{k} \bar{V} - \mu_1 \nabla^4 \bar{V} + p g \cos \alpha^* \end{aligned} \quad 11$$

$$\rho C_P \left(\frac{\partial}{\partial \bar{t}} + \bar{U} \frac{\partial}{\partial \bar{X}} + \bar{V} \frac{\partial}{\partial \bar{Y}} \right) \bar{T} = k' \left(\frac{\partial^2}{\partial \bar{t}^2} + \frac{\partial^2}{\partial \bar{X}^2} + \frac{\partial^2}{\partial \bar{Y}^2} \right) \bar{T} + \mu \left[\left(\frac{\partial \bar{U}}{\partial \bar{Y}} + \frac{\partial \bar{V}}{\partial \bar{X}} \right)^2 + 2 \left(\frac{\partial \bar{U}}{\partial \bar{X}} \right)^2 + \right. \\ \left. 2 \left(\frac{\partial \bar{V}}{\partial \bar{Y}} \right)^2 \right] \quad 12$$

$$\text{Let } \nabla^2 = \left(\frac{\partial^2}{\partial \bar{X}^2} + \frac{\partial^2}{\partial \bar{Y}^2} \right) \text{ then } \nabla^4 = (\nabla^2)^2$$

Where ρ is the fluid density, $\bar{V} = [\bar{U}, \bar{V}]$ is the velocity vector, \bar{P} is the hydrodynamic pressure, $\bar{S}_{\bar{X}\bar{X}}$, $\bar{S}_{\bar{X}\bar{Y}}$, and $\bar{S}_{\bar{Y}\bar{Y}}$ are the elements of the extra stress tensor \bar{S} , σ is the electrical conductivity, β_0 is the constant magnetic field, β is the inclination of the magnetic field, Ω is the rotation C_p is specific heat, k' is the thermal conductivity, \bar{T} is a temperature, and μ for viscosity.

Listed below are the parts of Powell-additional Eying's stress tensor, as described by Eq.5



$$\bar{S}_{XX} = 2 \left(\mu + \frac{1}{\beta c_1} \right) \bar{U}_X - \frac{1}{3\beta c_1^3} \left[2\bar{U}_X^2 + (\bar{V}_X + \bar{U}_Y)^2 + 2\bar{V}_Y^2 \right] \bar{U}_X \quad 13$$

$$\bar{S}_{XY} = 2 \left(\mu + \frac{1}{\beta c_1} \right) (\bar{V}_X + \bar{U}_Y) - \frac{1}{6\beta c_1^3} \left[2\bar{U}_X^2 + (\bar{V}_X + \bar{U}_Y)^2 + 2\bar{V}_Y^2 \right] (\bar{V}_X + \bar{U}_Y) \quad 14$$

$$\bar{S}_{YY} = 2 \left(\mu + \frac{1}{\beta c_1} \right) \bar{V}_Y - \frac{1}{3\beta c_1^3} \left[2\bar{U}_X^2 + (\bar{V}_X + \bar{U}_Y)^2 + 2\bar{V}_Y^2 \right] \bar{V}_Y \quad 15$$

Natural peristaltic motion is an erratic occurrence, but it applying the transformation from laboratory frame, stability can be assumed (fixed frame) (\bar{X}, \bar{Y}) to wave frame (move frame) (\bar{x}, \bar{y}) . The subsequent transformations determine the relationship between coordinates, velocities, and pressure in laboratory frame (\bar{X}, \bar{Y}) to wave frame (\bar{x}, \bar{y})

$$\bar{x} = \bar{X} - c, \bar{y} = \bar{Y}, \bar{u} = \bar{U} - c, \bar{v} = \bar{V}, \bar{p}(\bar{x}, \bar{y}) = \bar{P}(\bar{X}, \bar{Y}, \bar{t}) \quad 16$$

Where \bar{u} and \bar{v} represent the velocity factors and \bar{p} represents the pressure in the wave frame. Now that Eq.15 has been substituted into Eqs.1, 2, and 9–14, the resulting equation has been normalized using the non-dimensional variables shown below:

$$x = \frac{1}{\lambda} \bar{x}, \quad y = \frac{1}{d} \bar{y}, \quad u = \frac{1}{c} \bar{u}, \quad v = \frac{1}{\delta c} \bar{v}, \quad p = \frac{d^2}{\lambda \mu c} \bar{p}, \quad t = \frac{c}{\lambda} \bar{t}, \quad h_1 = \frac{1}{d} \bar{h}_1, \\ h_2 = \frac{1}{d} \bar{h}_2,$$

$$Ha = d \sqrt{\frac{\sigma}{\mu}} \beta_0, \quad Da = \frac{\bar{k}}{d^2}, \quad w = \frac{1}{\mu \beta c_1}, \quad A = \frac{w}{6} \left(\frac{c}{c_1 d} \right)^2, \quad \bar{T} = T - T_0, \quad \theta = \frac{T - T_0}{T_1 - T_0},$$

$$Fr = \frac{c^2}{dg}, \quad \beta_1 = \frac{\beta^*}{d},$$

$$S_{xx} = \frac{\lambda}{\mu c} \bar{S}_{XX}, \quad S_{xy} = \frac{d}{\mu c} \bar{S}_{XY}, \quad S_{yy} = \frac{d}{\mu c} \bar{S}_{YY} \quad 17$$

$$\delta = \frac{d}{\lambda}, \quad Re = \frac{\rho c d}{\mu},$$

Where, (δ) is the wave number, (h_1) and (h_2) are non-dimensional lower and upper wall surface respectively, (Re) is the Reynolds number, (Ha) is the Hartman number, (Φ) is the amplitude ratio, (w) is the non-dimensional permeability of the porous medium parameter, (Da) is the Darcy number, (A) is the Powell-Eyring fluid parameter, (T_0) and (T_1) are the temperatures at



the upper and lower walls, (Fr) is the Froude number, and (α^*) inclination angle of the channel to the horizontal axis.

Following that is

$$h_1(x, t) = 1 - a \sin(2\pi x), \quad a = \frac{a_1}{d} \quad 18$$

$$h_2(x, t) = -d^* - b \sin(2\pi x + \Phi), \quad b = \frac{a_2}{d}, \quad d^* = \frac{d'}{d} \quad 19$$

Where a , b , d^* , and satisfy Eq.3, then

$$a^2 + b^2 + 2ab \cos \Phi \leq (1 + d^*)^2 \quad 20$$

$$\frac{\partial u}{\partial x} + \frac{\partial v}{\partial y} = 0 \quad 21$$

$$\begin{aligned} Re\delta \left(\frac{\partial u}{\partial t} + u \frac{\partial u}{\partial x} + v \frac{\partial u}{\partial y} \right) - \frac{\rho d^2 \Omega}{\mu} \left(\Omega u + 2 \frac{\delta c}{d} \frac{\partial v}{\partial t} \right) \\ = -\frac{\partial p}{\partial x} + \delta^2 \frac{\partial}{\partial x} S_{xx} + \frac{\partial}{\partial y} S_{xy} \\ - Ha^2 \cos \beta (u \cos \beta - \delta v \sin \beta) - \frac{1}{Da} u - \frac{1}{\alpha^2} \left(\delta^4 \frac{\partial^4}{\partial x^4} + 2\delta^2 \frac{\partial^4}{\partial x^2 \partial y^2} + \right. \\ \left. \frac{\partial^4}{\partial y^4} \right) u + \frac{Re}{Fr} \sin \alpha^* \end{aligned} \quad 22$$

$$\begin{aligned} Re\delta^3 \left(\frac{\partial v}{\partial t} + u \frac{\partial v}{\partial x} + v \frac{\partial v}{\partial y} \right) - \frac{\rho d^2 \Omega \delta}{\mu} \left(\Omega \delta v + 2 \frac{\delta c}{d} \frac{\partial v}{\partial t} \right) \\ = -\frac{\partial p}{\partial x} + \delta^2 \frac{\partial}{\partial x} S_{xy} + \delta \frac{\partial}{\partial y} S_{yy} \\ + Ha^2 \sin \beta (\delta u \cos \beta - \delta^2 v \sin \beta) - \delta^2 \frac{1}{Da} v - \frac{\delta^2}{\alpha^2} \left(\delta^4 \frac{\partial^4}{\partial x^4} + \right. \\ \left. 2\delta^2 \frac{\partial^4}{\partial x^2 \partial y^2} + \frac{\partial^4}{\partial y^4} \right) v + \delta \frac{Re}{Fr} \cos \alpha^* \end{aligned} \quad 23$$

$$\begin{aligned} Re\delta \left(\frac{\partial \theta}{\partial t} + u \frac{\partial \theta}{\partial x} + v \frac{\partial \theta}{\partial y} \right) = \frac{1}{Pr} \left(c^2 \delta^2 \frac{\partial^2 \theta}{\partial t^2} + \delta^2 \frac{\partial^2 \theta}{\partial x^2} + \frac{\partial^2 \theta}{\partial y^2} \right) + Ec \left[\left(\frac{\partial u}{\partial y} + \right. \right. \\ \left. \left. \delta^2 \frac{\partial v}{\partial x} \right)^2 + 2\delta^2 \left(\frac{\partial u}{\partial x} \right)^2 + 2\delta^2 \left(\frac{\partial v}{\partial y} \right)^2 \right] \quad 24 \end{aligned}$$



$$S_{xx} = 2(1 + w) \frac{\partial u}{\partial x} - 2A \left[2\delta^2 \left(\frac{\partial u}{\partial x} \right)^2 + \left(\frac{\partial u}{\partial y} + \delta^2 \frac{\partial v}{\partial x} \right)^2 + 2\delta^2 \left(\frac{\partial v}{\partial y} \right)^2 \right] \frac{\partial u}{\partial x} \quad 25$$

$$S_{xy} = (1 + w) \left(\delta^2 \frac{\partial v}{\partial x} + \frac{\partial u}{\partial y} \right) - A \left[2\delta^2 \left(\frac{\partial u}{\partial x} \right)^2 + \left(\frac{\partial u}{\partial y} + \delta^2 \frac{\partial v}{\partial x} \right)^2 + 2\delta^2 \left(\frac{\partial v}{\partial y} \right)^2 \right] \left(\delta^2 \frac{\partial v}{\partial x} + \frac{\partial u}{\partial y} \right) \quad 26$$

$$S_{yy} = 2(1 + w) \left(\delta \frac{\partial v}{\partial y} \right) - 2A\delta \left[2\delta^2 \left(\frac{\partial u}{\partial x} \right)^2 + \left(\frac{\partial u}{\partial y} + \delta^2 \frac{\partial v}{\partial x} \right)^2 + 2\delta^2 \left(\frac{\partial v}{\partial y} \right)^2 \right] \quad 27$$

In previous equations, Pr is Prandtl number, Ec is Eckert number and θ is the dimensionless temperature.

Following are the relations between the stream function (ψ) and velocity components:

$$u = \frac{\partial \psi}{\partial y}, v = -\frac{\partial \psi}{\partial x} \quad 28$$

Substituting Eq.28 into Eqs. 21 to 27, noting that the mass balance displayed by Eq.21 similarly satisfied, produces the consequence that Eq.28 is satisfied.

$$Re \delta \left(\frac{\partial^2 \psi}{\partial t \partial y} + \frac{\partial^3 \psi}{\partial x \partial y^2} - \frac{\partial^3 \psi}{\partial x \partial y^2} \right) - \frac{\rho d^2 \Omega}{\mu} \left(\Omega \frac{\partial \psi}{\partial y} - 2 \frac{\delta c}{d} \frac{\partial^2 \psi}{\partial t \partial x} \right) = -\frac{\partial p}{\partial x} + \delta^2 \frac{\partial}{\partial x} S_{xx} + \frac{\partial}{\partial y} S_{xy} - Ha^2 \cos \beta \left(\frac{\partial \psi}{\partial y} \cos \beta + \delta \frac{\partial \psi}{\partial x} \sin \beta \right) - \frac{1}{Da} \frac{\partial \psi}{\partial y} - \frac{1}{\alpha^2} \left(\delta^4 \frac{\partial^4}{\partial x^4} + 2\delta^2 \frac{\partial^4}{\partial x^2 \partial y^2} + \frac{\partial^4}{\partial y^4} \right) \frac{\partial \psi}{\partial y} + \frac{Re}{Fr} \sin \alpha^* \quad 29$$

$$Re \delta^3 \left(-\frac{\partial^2 \psi}{\partial t \partial x} - \frac{\partial^3 \psi}{\partial x^2 \partial y} - \frac{\partial^3 \psi}{\partial x^2 \partial y} \right) - \frac{\rho d^2 \Omega \delta}{\mu} \left(-\Omega \delta \frac{\partial \psi}{\partial x} - 2 \frac{\delta c}{d} \frac{\partial^2 \psi}{\partial t \partial x} \right) = -\frac{\partial p}{\partial y} + \delta^2 \frac{\partial}{\partial x} S_{xy} + \delta \frac{\partial}{\partial y} S_{yy} + Ha^2 \sin \beta \left(\delta \frac{\partial \psi}{\partial y} \cos \beta + \delta^2 \frac{\partial \psi}{\partial x} \sin \beta \right) + \delta^2 \frac{1}{Da} \frac{\partial \psi}{\partial x} + \frac{\delta^2}{\alpha^2} \left(\delta^4 \frac{\partial^4}{\partial x^4} + 2\delta^2 \frac{\partial^4}{\partial x^2 \partial y^2} + \frac{\partial^4}{\partial y^4} \right) \frac{\partial \psi}{\partial x} + \delta \frac{Re}{Fr} \cos \alpha^* \quad 30$$



$$Re\delta \left(\frac{\partial \theta}{\partial t} + \frac{\partial \Psi}{\partial y} \frac{\partial \theta}{\partial x} - \frac{\partial \Psi}{\partial x} \frac{\partial \theta}{\partial y} \right) = \frac{1}{Pr} \left(c^2 \delta^2 \frac{\partial^2 \theta}{\partial t^2} + \delta^2 \frac{\partial^2 \theta}{\partial x^2} + \frac{\partial^2 \theta}{\partial y^2} \right) + Ec \left[\left(\frac{\partial^2 \Psi}{\partial y^2} + \delta^2 \frac{\partial^2 \Psi}{\partial x^2} \right)^2 + 2\delta^2 \left(\frac{\partial^2 \Psi}{\partial x \partial y} \right)^2 + 2\delta^2 \left(\frac{\partial^2 \Psi}{\partial x \partial y} \right)^2 \right] \quad 31$$

$$S_{xx} = 2(1 + w) \frac{\partial^2 \Psi}{\partial x \partial y} - 2A \left[2\delta^2 \left(\frac{\partial^2 \Psi}{\partial x \partial y} \right)^2 + \left(\frac{\partial^2 \Psi}{\partial y^2} - \delta^2 \frac{\partial^2 \Psi}{\partial x^2} \right)^2 + 2\delta^2 \left(\frac{\partial^2 \Psi}{\partial x \partial y} \right)^2 \right] \quad 32$$

$$S_{xy} = (1 + w) \left(-\delta^2 \frac{\partial^2 \Psi}{\partial x^2} + \frac{\partial^2 \Psi}{\partial y^2} \right) - A \left[2\delta^2 \left(\frac{\partial^2 \Psi}{\partial x \partial y} \right)^2 + \left(-\delta^2 \frac{\partial^2 \Psi}{\partial x^2} + \frac{\partial^2 \Psi}{\partial y^2} \right)^2 + 2\delta^2 \left(\frac{\partial^2 \Psi}{\partial x \partial y} \right)^2 \right] \left(-\delta^2 \frac{\partial^2 \Psi}{\partial x^2} + \frac{\partial^2 \Psi}{\partial y^2} \right) \quad 33$$

$$S_{yy} = -2(1 + w) \delta \frac{\partial^2 \Psi}{\partial x \partial y} - 2A \delta \left[2\delta^2 \left(\frac{\partial^2 \Psi}{\partial x \partial y} \right)^2 + \left(\frac{\partial^2 \Psi}{\partial y^2} - \delta^2 \frac{\partial^2 \Psi}{\partial x^2} \right)^2 + 2\delta^2 \left(\frac{\partial^2 \Psi}{\partial x \partial y} \right)^2 \right] \left(-\frac{\partial^2 \Psi}{\partial x \partial y} \right) \quad 34$$

$$-\frac{\rho d^2 \Omega^2}{\mu} \frac{\partial \Psi}{\partial y} = -\frac{\partial p}{\partial x} + \frac{\partial}{\partial y} S_{xy} - \left(Ha^2 \cos^2 \beta + \frac{1}{Da} \right) \frac{\partial \Psi}{\partial y} - \frac{1}{\alpha^2} \frac{\partial^5 \Psi}{\partial y^5} + \frac{Re}{Fr} \sin \alpha^* \quad 35$$

$$-\frac{\partial p}{\partial y} = 0 \quad 36$$

$$\frac{\partial^2 \theta}{\partial y^2} = -Ec.Pr \left(\frac{\partial^2 \Psi}{\partial y^2} \right)^2 \quad 37$$

Now, the Eqs.29- 34 become the form when (Re and $\delta \ll 1$) are present:

While the component of the extra stress tensor becomes the form of

$$S_{xx} = 2(1 + w) \frac{\partial^2 \Psi}{\partial x \partial y} - 2A \left(\frac{\partial^2 \Psi}{\partial y^2} \right)^2 \frac{\partial^2 \Psi}{\partial x \partial y} \quad 38$$

$$S_{xy} = (1 + w) \left(\frac{\partial^2 \Psi}{\partial y^2} \right) - A \left(\frac{\partial^2 \Psi}{\partial y^2} \right)^3 \quad 39$$

$$S_{yy} = 0 \quad 40$$



Also, if Eq.39 is entered into Eq.35 as well as the derivative with regard to y and by $(w+1)$ is taken, then the following equation is obtained:

$$\frac{\partial^4 \Psi}{\partial y^4} - \eta A \frac{\partial^2}{\partial y^2} \left(\frac{\partial^2 \Psi}{\partial y^2} \right)^3 - \zeta \frac{\partial^2 \Psi}{\partial y^2} - \eta \frac{1}{\alpha^2} \frac{\partial^6 \Psi}{\partial y^6} = 0 \quad 41$$

Where

$$\zeta = \frac{Ha^2 \cos^2 \beta + \frac{1}{Da} \frac{\rho d^2 \Omega^2}{\mu}}{w+1}, \quad \eta = \frac{1}{w+1}$$

In the wave frame, the dimensionless volume flow rate and boundary

$$\Psi = \frac{F}{2}, \frac{\partial \Psi}{\partial y} = -1, \theta = 0 \quad \text{at } y = h_1, \quad \Psi = -\frac{F}{2}, \frac{\partial \Psi}{\partial y} = -1, \theta = 0 \quad \text{at } y = h_2 \quad 42$$

$$\frac{\partial \Psi}{\partial y} + \beta_1 \frac{\partial^2 \Psi}{\partial y^2} = -1 \quad \text{at } y = h_1, \quad \frac{\partial \Psi}{\partial y} + \beta_1 \frac{\partial^2 \Psi}{\partial y^2} = -1 \quad \text{at } y = h_2 \quad 43$$

$$\frac{\partial^3 \Psi}{\partial y^3} = 0 \quad \text{at } y = h_1, \quad \frac{\partial^3 \Psi}{\partial y^3} = 0 \quad \text{at } y = h_2 \quad 44$$

condition are as follows:

F represents the dimensionless temporal average flow in the wave frame.

Through the expression, it is related to the dimensionless temporal mean flow rate (Q) in the laboratory frame

$$Q = F + 1 + d^* \quad 45$$

3. Effect of a couple – stress

In this part, a relationship between the pair stress parameter (α) and the material fluid parameters (A) would be found. The relationship will aid us in simplifying the problem's solution strategy. In order to see the impact of every parameter contained in the problem, the zero and first-order solutions must be found. However, we just need to find the zero-order utilizing the relationship between the pair stress parameter and the material fluid properties. Fluid parameters from a substance with no dimensions:

$$\text{Let } A = \frac{w}{6} \left(\frac{c}{c_1 d} \right)^2$$

Then

$$d = \sqrt{\frac{w}{6A}} \left(\frac{c}{c_1} \right) \quad 46$$

Since



$$\alpha = d \sqrt{\frac{\mu}{\mu_1}} \quad 47$$

Substitute Eq. (46) into Eq. (47), we get

$$\alpha = \sqrt{\frac{w\mu}{6A\mu_1}} \left(\frac{c}{c_1}\right) \quad 48$$

$$\alpha^2 = \frac{w\mu}{6A\mu_1} \left(\frac{c}{c_1}\right)^2 \quad \text{and} \quad \frac{1}{\alpha^2} = \frac{6A\mu_1}{w\mu} \left(\frac{c_1}{c}\right)^2 \quad 49$$

4. Solution of the problem

By using Eq.45 with Eqs.35 – 40 and boundary conditions (42 – 44) and since $\delta \leq 1$, and using the approximation of a long wavelength and a low Reynolds number. For the appearance of the couple stress parameter in the equation, the solution is limited to the zero order by giving all the parameters required to solve the problem and find the results, we get the

$$\Psi_{yyyy} - \zeta\Psi_{yy} - \frac{\eta}{\alpha^2}\Psi_{yyyyyy} = 0 \quad 50$$

motion equation in the terms of stream function which is

The solution of the momentum equation is straight forward and can be written as

$$\Psi = \sqrt{2} \left(\frac{\sqrt{2}e^{-\frac{y\sqrt{\alpha^2 - \sqrt{\alpha^2(\alpha^2 - 4\zeta\eta)}}{\eta}}}{\sqrt{2}} C_1 + \frac{\sqrt{2}e^{-\frac{y\sqrt{\alpha^2 - \sqrt{\alpha^2(\alpha^2 - 4\zeta\eta)}}{\eta}}}{\sqrt{2}} C_2 + \frac{\sqrt{2}e^{-\frac{y\sqrt{\alpha^2 + \sqrt{\alpha^2(\alpha^2 - 4\zeta\eta)}}{\eta}}}{\sqrt{2}} C_3 + \frac{\sqrt{2}e^{-\frac{y\sqrt{\alpha^2 + \sqrt{\alpha^2(\alpha^2 - 4\zeta\eta)}}{\eta}}}{\sqrt{2}} C_4 \right) + C_5 + yC_6 \quad 51$$

Within the fixed frame, the axial velocity component is expressed as



$$u(x, y, t) = \Psi_y \quad 52$$

It is possible to rewrite Eq.35 as

$$\frac{\partial p}{\partial x} = (w + 1)\Psi_{yyy} - (w + 1)\zeta\Psi_y - \frac{1}{\alpha^2}\Psi_{yyyyy} + \frac{Re}{Fr}\sin\alpha^* \quad 55$$

5. Energy equation solution

The solution of Eq.37 with boundary conditions

$$\theta = 0 \text{ at } y = h_1 \text{ and } \theta = 1 \text{ at } y = h_2 \quad 56$$

$$\begin{aligned} \theta = & -\frac{1}{p_3^2 p_4^2} 2Ecpr \left(\frac{1}{2} C_4^2 e^{-2p_2 y} p_2^2 p_3^2 + \frac{1}{2} C_3^2 e^{2p_2 y} p_2^2 p_3^2 + \right. \\ & \frac{4C_2 C_3 e^{-(p_1-p_2)y} p_1^2 p_2^2 p_3 p_4}{(p_1-p_2)^2} + \frac{4C_1 C_4 e^{(p_1-p_2)y} p_1^2 p_2^2 p_3 p_4}{(p_1-p_2)^2} + \\ & \frac{4C_2 C_4 e^{-(p_1+p_2)y} p_1^2 p_2^2 p_3 p_4}{(p_1+p_2)^2} + \frac{4C_1 C_3 e^{(p_1+p_2)y} p_1^2 p_2^2 p_3 p_4}{(p_1+p_2)^2} + \frac{1}{2} C_2^2 e^{-2p_1 y} p_1^2 p_4^2 + \\ & \left. \frac{1}{2} C_1^2 e^{2p_1 y} p_1^2 p_4^2 + 2C_3 C_4 p_2^4 p_3^2 y^2 + 2C_1 C_2 p_1^4 p_4^2 y^2 \right) + r_1 + y r_2 \quad 57 \end{aligned}$$

Where

$$p_1 = \sqrt{\frac{\alpha^2 - \sqrt{\alpha^2 (\alpha^2 - 4\zeta\eta)}}{\eta}} / \sqrt{2}$$

$$p_2 = \sqrt{\frac{\alpha^2 + \sqrt{\alpha^2 (\alpha^2 - 4\zeta\eta)}}{\eta}} / \sqrt{2}$$

$$p_3 = \sqrt{\frac{\alpha^2 - \sqrt{\alpha^2 (\alpha^2 - 4\zeta\eta)}}{\eta}} \quad \sqrt{\frac{\alpha^2 - \sqrt{\alpha^4 - 4\alpha^2 \zeta\eta}}{\eta}}$$

$$p_4 = \sqrt{\frac{\alpha^2 + \sqrt{\alpha^2 (\alpha^2 - 4\zeta\eta)}}{\eta}} \quad \sqrt{\frac{\alpha^2 + \sqrt{\alpha^4 - 4\alpha^2 \zeta\eta}}{\eta}}$$

It is possible to prove that r_1 and r_2 are constants using the boundary conditions, and can be stated θ as in the index.

6. Results and discussions



This section consists of three subsections. In the first, the velocity is discussed, while in the second, the pressure gradient is displayed, and in the third, the temperature distribution is illustrated using the MATHEMATICA software.

❖ Velocity u :

Case variation of u indicates the variance in axial velocity across the channel. The influence of various values (Ha , β , Da , Ω , w , ϕ , β_1 , α) on the axial velocity u is illustrated in Figs. 2 -9

- Figs. 2, 4, and 8 display the increases in the values of Hartman number (Ha), the inclination of magnetic field (β), slip condition (β_1) there is no effect on the axial velocity in the central region of the channel, whereas the axial velocity is rising close to the channel wall's margin.
- Figs. 5, 6, 7, and 9 illustrate that increases in the values of the rotation (Ω), the values of porous medium parameter (w), the amplitude ratio (ϕ), and couple stress parameter (α) have no effect on the axial velocity in the channel's central region, whereas the axial velocity decreases near the channel wall.
- The axial velocity does not change as the values of Darcy number (Da) values increase, as shown in Fig. 3.

❖ Pressure gradient dp/dx :

Case variation of dp/dx indicates the variance in axial Pressure gradient across the channel. The influence of various values (Ha , β , Da , d , w , Ω , ϕ , α , α^* , Fr , Re , β_1) on the Pressure gradient dp/dx is illustrated in Figs. 10 - 21

- Figs. 10 and 14 demonstrate that increases in the values of the Hartman number (Ha) and the porous medium parameter (w) cause decrease the curve of the pressure gradient.
- Figs. 11, 13, 15, 17, and 21 the increases in the inclination of magnetic field (β), width of the channel (d), the rotation (Ω), couple stress parameter (α), and slip condition (β_1) lead to increases the curve of the pressure gradient .
- Figs. 12, 18, 19, and 20 demonstrate that the pressure gradient does not change as values increase the Darcy number (Da), the inclination angle of



the channel to the horizontal axis (α^*), the Reynolds number (Re), and the Froude number (Fr).

• Fig. 16 for approximately $-4.2 < x < -1.2$ the pressure gradient increases as the amplitude ratio increases (ϕ), but for approximately $x > -1.2$ and $x < -4.2$, the pressure gradient decreases.

❖ Temperature distribution θ :

The effect of relevant parameters on the temperature distribution θ is graphically illustrated in Figs.22-34

where as depicted in the following figures

- Figs. 22, 26, 27, 28, 29 and 30 illustrate that increases in the values of the Hartman number (Ha), the porous medium parameter (w), the amplitude ratio (ϕ), couple stress parameter (α), the Eckert number (Ec), and the Prandtl number (Pr) have no effect on the temperature field in the channel's central region, whereas the temperature field decreases near the channel wall.
- Figs. 24, and 34 display the increases in the values of the inclination of magnetic field (β) and the slip condition (β_1) there is no effect on the temperature field in the central region of the channel, whereas the temperature field is rising close to the channel wall's margin.
- The temperature field does not change as the Darcy number (Da), the rotation (Ω), the Reynolds number (Re), the Froude number (Fr), and the inclination angle of the channel to the horizontal axis (α^*) values increase, as shown in Figs. 23, 25, 31, 32 and 33.

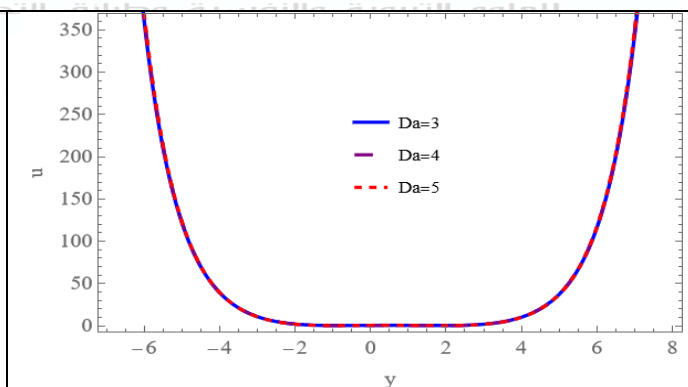
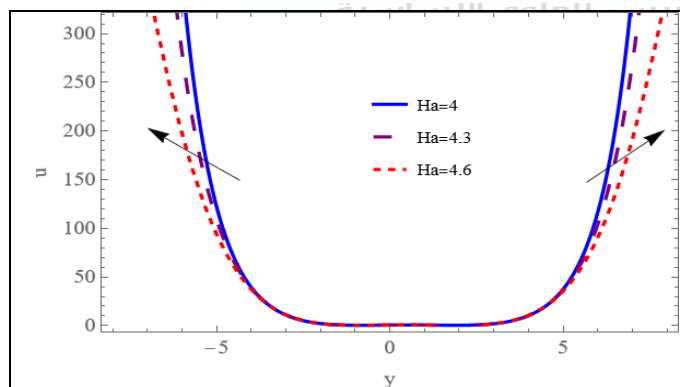


Figure 2: Velocity variation for different (Ha) when $Ha = 4, \beta = 2.5, Da = 3, \rho = 0.7, d = 5, \Omega = 1.5, \mu = 3, w = 0.01, \phi = 2.5, a = 0.4, b = 0.6, d_1 = 0.5, F_0 =$

Figure 3: Velocity variation for different (Da) when $Ha = 4, \beta = 2.5, Da = 3, \rho = 0.7, d = 5, \Omega = 1.5, \mu = 3, w = 0.01, \phi = 2.5, a = 0.4, b = 0.6, d_1 = 0.5, F_0 =$



$0.9, \beta_1 = 4, \alpha = 0.6$

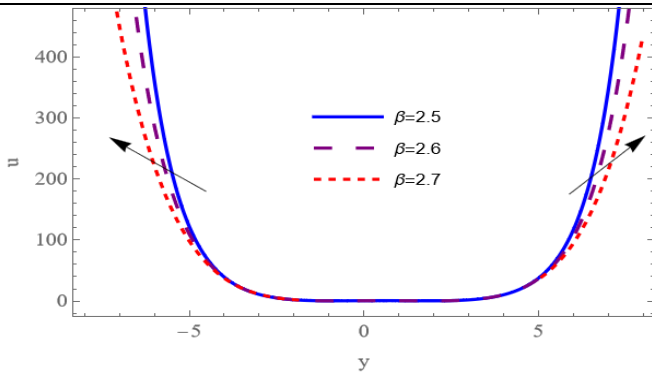


Figure 4: Velocity variation for different (β) when $Ha = 4, \beta = 2.5, Da = 3, \rho = 0.7, d = 5, \Omega = 1.5, \mu = 3, w = 0.01, \phi = 2.5, a = 0.4, b = 0.6, d_1 = 0.5, F_0 = 0.9, \beta_1 = 4, \alpha = 0.6$

$0.9,$

$\beta_1 = 4, \alpha = 0.6$

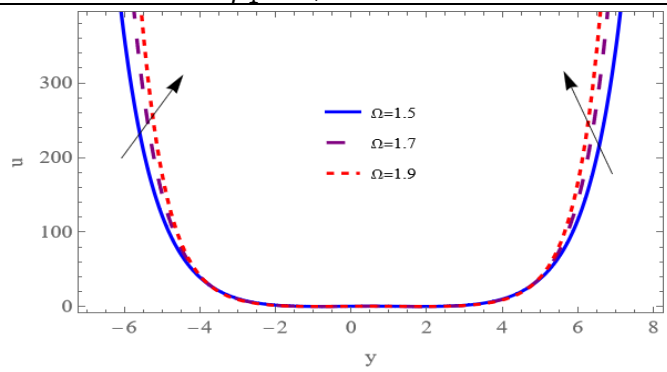


Figure 5: Velocity variation for different (Ω) when $Ha = 4, \beta = 2.5, Da = 3, \rho = 0.7, d = 5, \Omega = 1.5, \mu = 3, w = 0.01, \phi = 2.5, a = 0.4, b = 0.6, d_1 = 0.5, F_0 = 0.9, \beta_1 = 4, \alpha = 0.6$

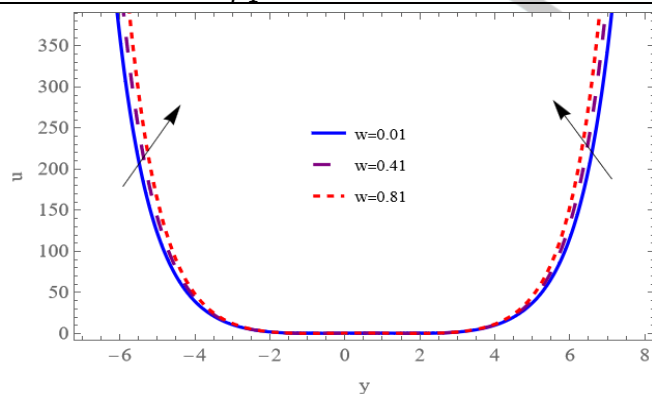


Figure 6: Velocity variation for different (w) when $Ha = 4, \beta = 2.5, Da = 3, \rho = 0.7, d = 5, \Omega = 1.5, \mu = 3, w = 0.01, \phi = 2.5, a = 0.4, b = 0.6, d_1 = 0.5, F_0 = 0.9, \beta_1 = 4, \alpha = 0.6$

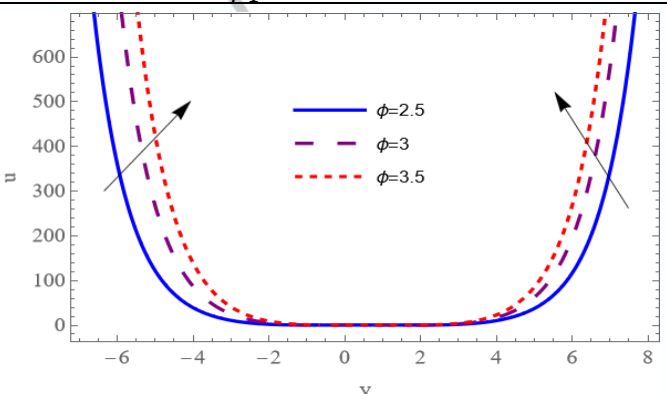


Figure 7: Velocity variation for different (ϕ) when $Ha = 4, \beta = 2.5, Da = 3, \rho = 0.7, d = 5, \Omega = 1.5, \mu = 3, w = 0.01, \phi = 2.5, a = 0.4, b = 0.6, d_1 = 0.5, F_0 = 0.9, \beta_1 = 4, \alpha = 0.6$

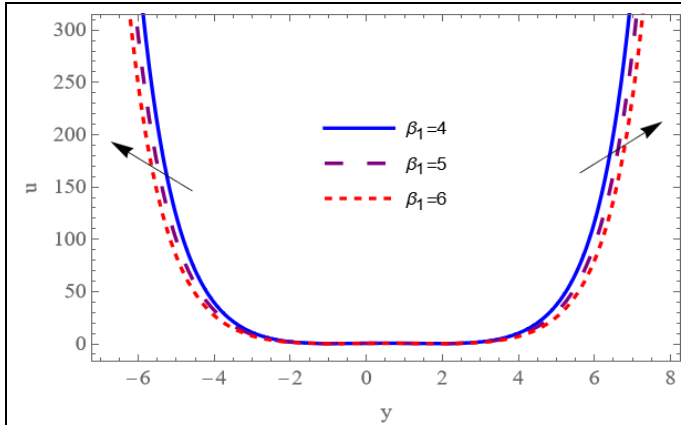


Figure 8: Velocity variation for different (β_1) when $Ha = 4, \beta = 2.5, Da = 3, \rho = 0.7, d = 5, \Omega = 1.5, \mu = 3, w = 0.01, \phi = 2.5, a = 0.4, b = 0.6, d_1 = 0.5, F_0 = 0.9, \beta_1 = 4, \alpha = 0.6$

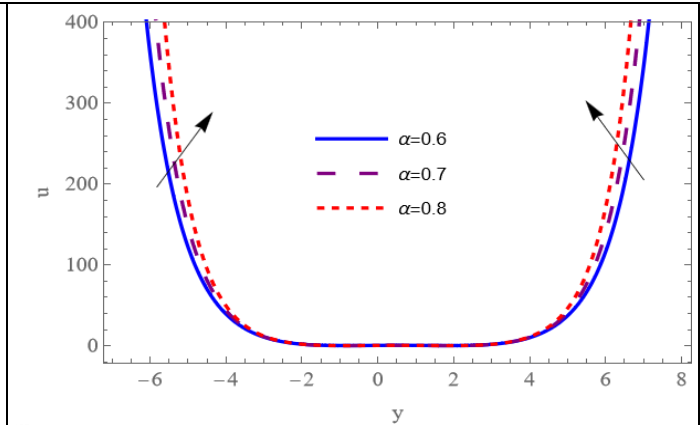


Figure 9: Velocity variation for different (α) when $Ha = 4, \beta = 2.5, Da = 3, \rho = 0.7, d = 5, \Omega = 1.5, \mu = 3, w = 0.01, \phi = 2.5, a = 0.4, b = 0.6, d_1 = 0.5, F_0 = 0.9, \beta_1 = 4, \alpha = 0.6$

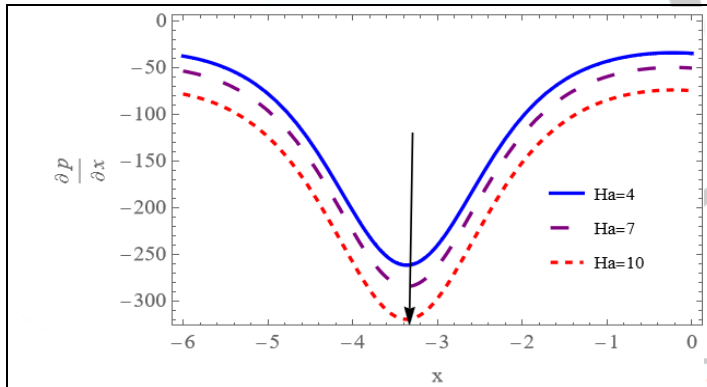


Figure 10: Pressure variation for different of (Ha) when $\beta = 2.5, Da = 3, \rho = 0.7, d = 5, \Omega = 1.5, \mu = 3, w = 0.01, \phi = 2.5, a = 0.4, b = 0.6, d_1 = 0.5, F_0 = 0.9, \alpha = 0.6, \alpha^* = 0.06, Re = 3, Fr = 3, \beta_1 = 0.1$

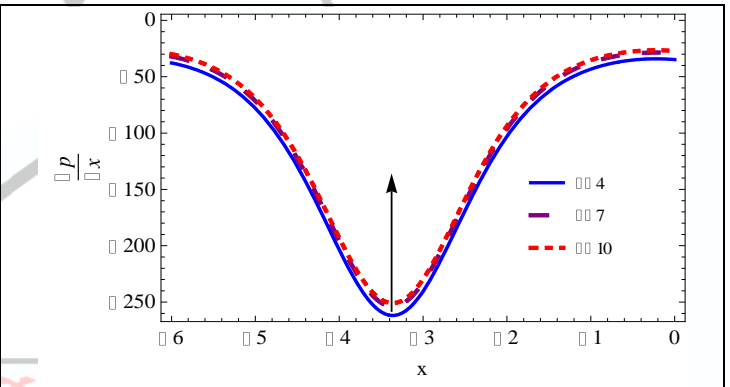


Figure 11: Pressure variation for different of (β) when $\beta = 2.5, Da = 3, \rho = 0.7, d = 5, \Omega = 1.5, \mu = 3, w = 0.01, \phi = 2.5, a = 0.4, b = 0.6, d_1 = 0.5, F_0 = 0.9, \alpha = 0.6, \alpha^* = 0.06, Re = 3, Fr = 3, \beta_1 = 0.1$

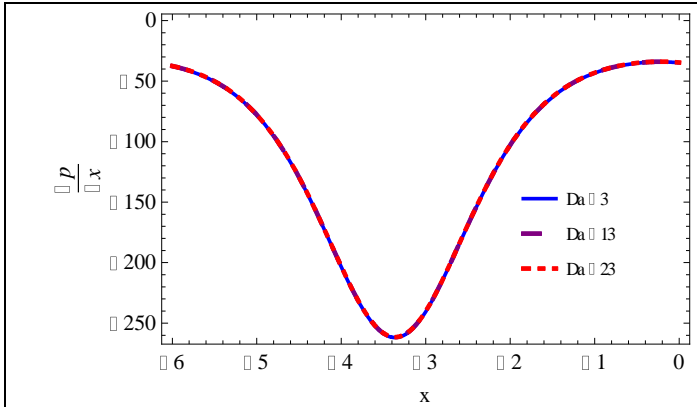


Figure 12: Pressure variation for different of (Da) when $\beta = 2.5, Da = 3, \rho = 0.7, d = 5, \Omega = 1.5, \mu = 3, w = 0.01, \phi = 2.5, a = 0.4, b = 0.6, d_1 = 0.5, F_0 = 0.9, \alpha = 0.6, \alpha^* = 0.06, Re = 3, Fr = 3, \beta_1 = 0.1$

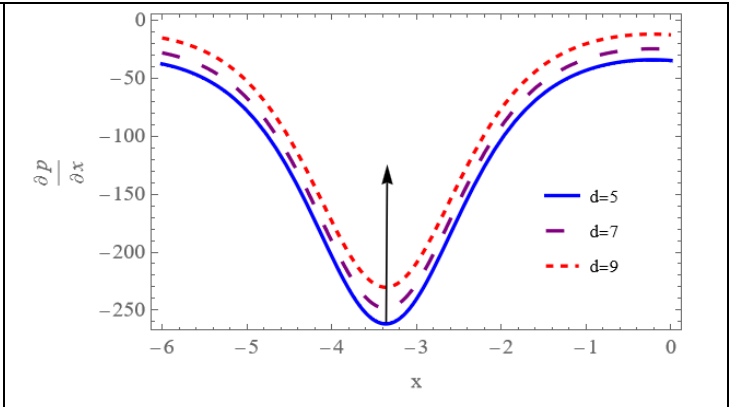


Figure 13: Pressure variation for different of (d) when $\beta = 2.5, Da = 3, \rho = 0.7, d = 5, \Omega = 1.5, \mu = 3, w = 0.01, \phi = 2.5, a = 0.4, b = 0.6, d_1 = 0.5, F_0 = 0.9, \alpha = 0.6, \alpha^* = 0.06, Re = 3, Fr = 3, \beta_1 = 0.1$

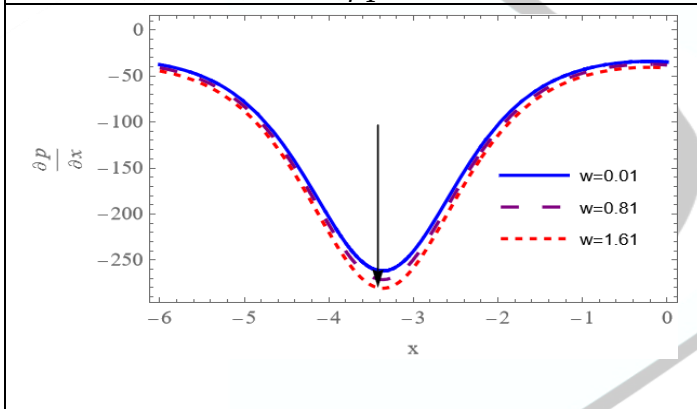


Figure 14: Pressure variation for different of (w) when $\beta = 2.5, Da = 3, \rho = 0.7, d = 5, \Omega = 1.5, \mu = 3, w = 0.01, \phi = 2.5, a = 0.4, b = 0.6, d_1 = 0.5, F_0 = 0.9, \alpha = 0.6, \alpha^* = 0.06, Re = 3, Fr = 3, \beta_1 = 0.1$

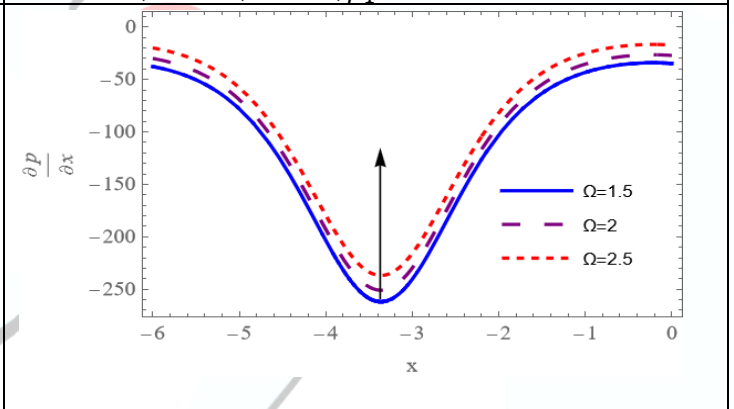


Figure 15: Pressure variation for different of (Ω) when $\beta = 2.5, Da = 3, \rho = 0.7, d = 5, \Omega = 1.5, \mu = 3, w = 0.01, \phi = 2.5, a = 0.4, b = 0.6, d_1 = 0.5, F_0 = 0.9, \alpha = 0.6, \alpha^* = 0.06, Re = 3, Fr = 3, \beta_1 = 0.1$

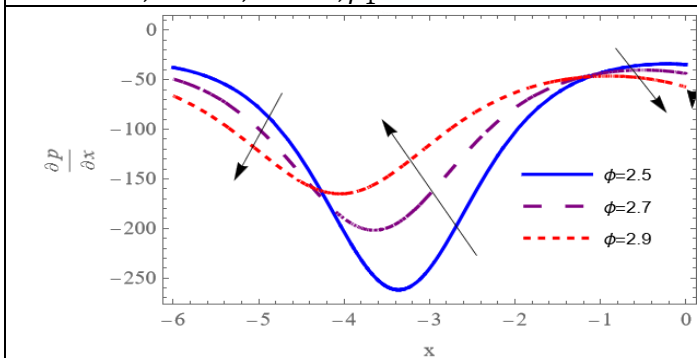


Figure 16: Pressure variation for different of (ϕ) when $\beta = 2.5, Da = 3, \rho = 0.7, d = 5, \Omega = 1.5, \mu = 3, w = 0.01, \phi = 2.5, a = 0.4,$

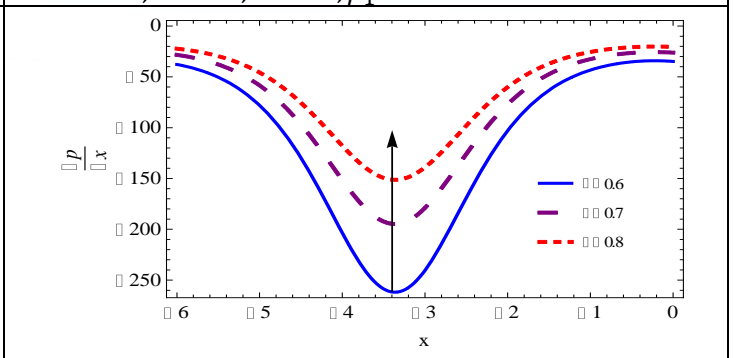


Figure 17: Pressure variation for different of (α) when $\beta = 2.5, Da = 3, \rho = 0.7, d = 5, \Omega = 1.5, \mu = 3, w = 0.01, \phi = 2.5, a = 0.4,$



$b = 0.6, d_1 = 0.5, F_0 = 0.9, \alpha = 0.6,$
 $\alpha^* = 0.06, Re = 3, Fr = 3, \beta_1 = 0.1$

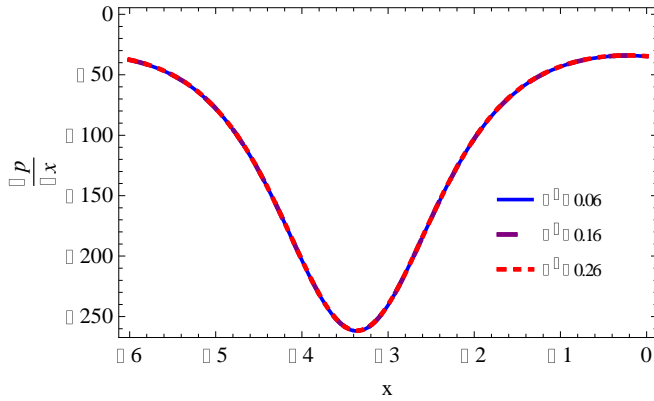


Figure 18: Pressure variation for different of (α^*) when $\beta = 2.5, Da = 3, \rho = 0.7, d = 5,$
 $\Omega = 1.5 \mu = 3, w = 0.01, \phi = 2.5, a = 0.4,$
 $b = 0.6, d_1 = 0.5, F_0 = 0.9, \alpha = 0.6,$
 $\alpha^* = 0.06, Re = 3, Fr = 3, \beta_1 = 0.1$

$b = 0.6, d_1 = 0.5, F_0 = 0.9, \alpha = 0.6,$
 $\alpha^* = 0.06, Re = 3, Fr = 3, \beta_1 = 0.1$

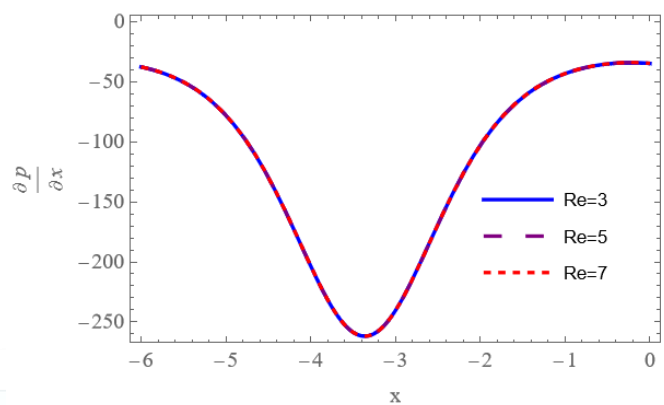


Figure 19: Pressure variation for different of (Re) when $\beta = 2.5, Da = 3, \rho = 0.7, d = 5,$
 $\Omega = 1.5 \mu = 3, w = 0.01, \phi = 2.5, a = 0.4,$
 $b = 0.6, d_1 = 0.5, F_0 = 0.9, \alpha = 0.6,$
 $\alpha^* = 0.06, Re = 3, Fr = 3, \beta_1 = 0.1$

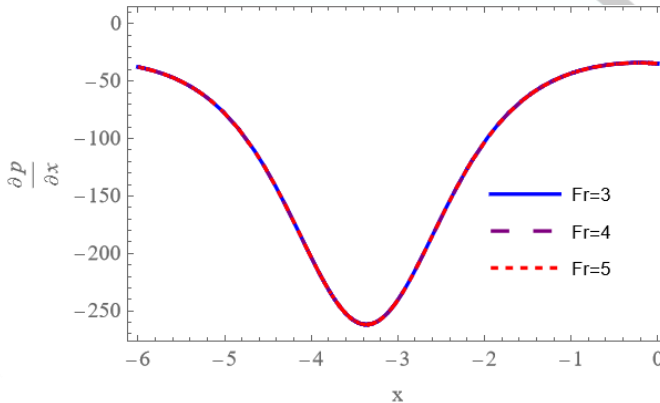


Figure 20: Pressure variation for different of (Fr) when $\beta = 2.5, Da = 3, \rho = 0.7, d = 5,$
 $\Omega = 1.5 \mu = 3, w = 0.01, \phi = 2.5, a = 0.4,$
 $b = 0.6, d_1 = 0.5, F_0 = 0.9, \alpha = 0.6,$
 $\alpha^* = 0.06, Re = 3, Fr = 3, \beta_1 = 0.1$

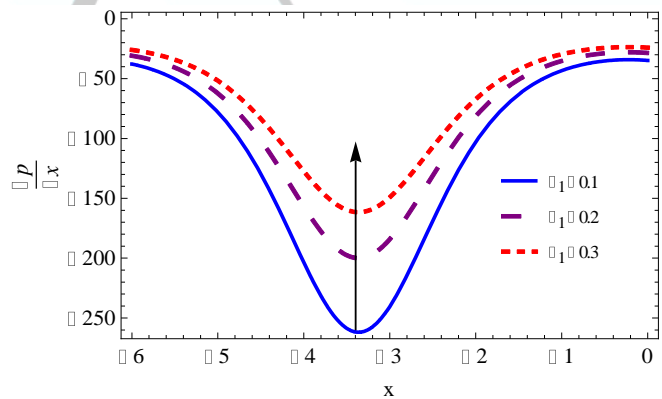


Figure 21: Pressure variation for different of (β_1) when $\beta = 2.5, Da = 3, \rho = 0.7, d = 5,$
 $\Omega = 1.5 \mu = 3, w = 0.01, \phi = 2.5, a = 0.4,$
 $b = 0.6, d_1 = 0.5, F_0 = 0.9, \alpha = 0.6,$
 $\alpha^* = 0.06, Re = 3, Fr = 3, \beta_1 = 0.1$

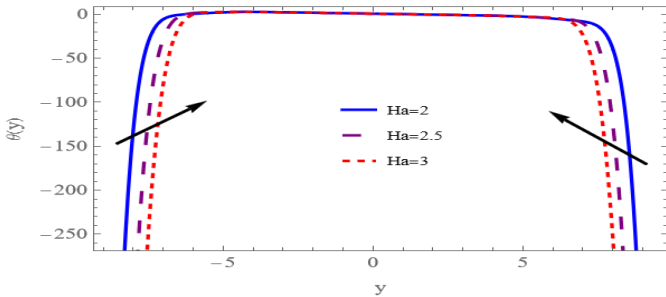


Figure 22: Variation of temperature θ with y for different value of (Ha) when $Ha = 2$,

$\beta = 0.1, Da = 10, \rho = 0.1, d = 0.5, \Omega = 0.5,$
 $\mu = 3, w = 0.3, \phi = 1.3, a = 0.2, b = 0.2,$
 $d_1 = 0.5, F_0 = 0.5, F_1 = 0, A = 0.1, \beta_1 = 4,$
 $Ec = 0.05, Pr = 0.05, \alpha = 0.6, Re = 2,$
 $Fr = 1, \alpha^* = 1.5$

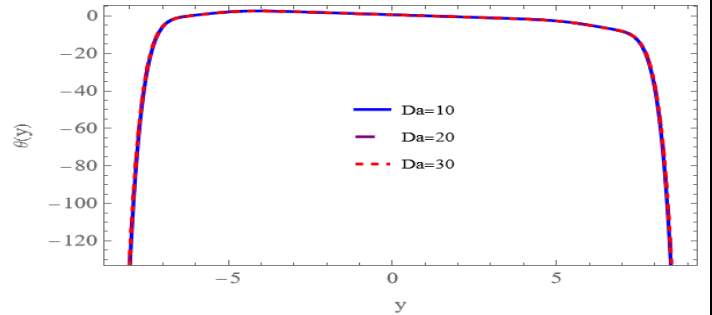


Figure 23 :Variation of temperature θ with y for different value of (Da) when $Ha = 2$,

$\beta = 0.1, Da = 10, \rho = 0.1, d = 0.5, \Omega = 0.5,$
 $\mu = 3, w = 0.3, \phi = 1.3, a = 0.2, b = 0.2,$
 $d_1 = 0.5, F_0 = 0.5, F_1 = 0, A = 0.1, \beta_1 = 4,$
 $Ec = 0.05, Pr = 0.05, \alpha = 0.6, Re = 2,$
 $Fr = 1, \alpha^* = 1.5$

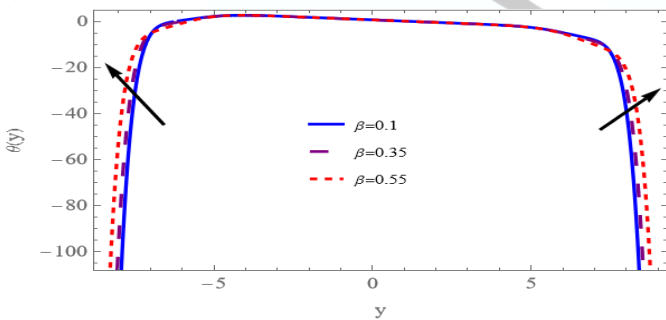


Figure 24:Variation of temperature θ with y for different value of (β) when $Ha = 2$,

$\beta = 0.1, Da = 10, \rho = 0.1, d = 0.5, \Omega = 0.5,$
 $\mu = 3, w = 0.3, \phi = 1.3, a = 0.2, b = 0.2,$
 $d_1 = 0.5, F_0 = 0.5, F_1 = 0, A = 0.1, \beta_1 = 4,$
 $Ec = 0.05, Pr = 0.05, \alpha = 0.6, Re = 2,$
 $Fr = 1, \alpha^* = 1.5$

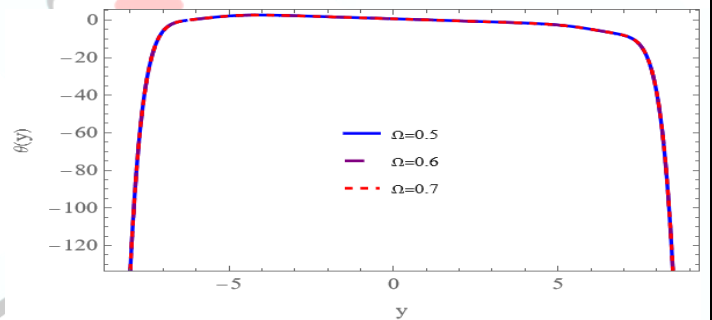


Figure 25:Variation of temperature θ with y for different value of (Ω) when $Ha = 2$,

$\beta = 0.1, Da = 10, \rho = 0.1, d = 0.5, \Omega = 0.5,$
 $\mu = 3, w = 0.3, \phi = 1.3, a = 0.2, b = 0.2,$
 $d_1 = 0.5, F_0 = 0.5, F_1 = 0, A = 0.1, \beta_1 = 4,$
 $Ec = 0.05, Pr = 0.05, \alpha = 0.6, Re = 2,$
 $Fr = 1, \alpha^* = 1.5$

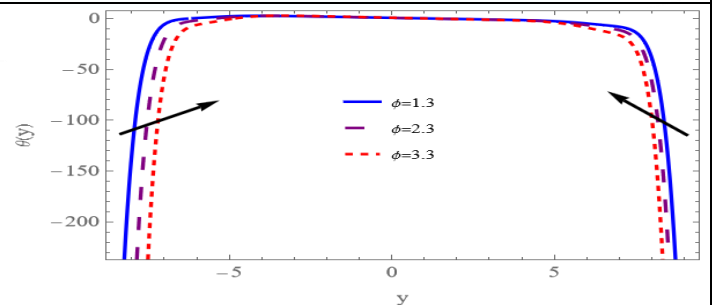
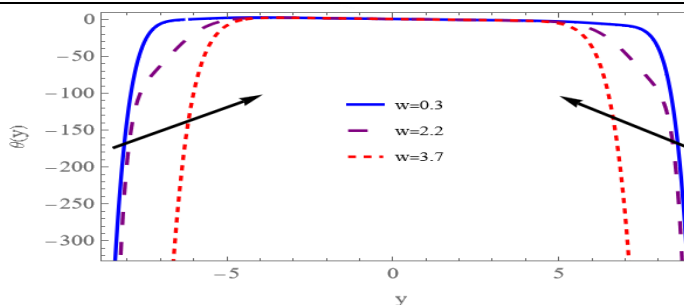




Figure 26: Variation of temperature θ with y for different value of (w) when $Ha = 2$,

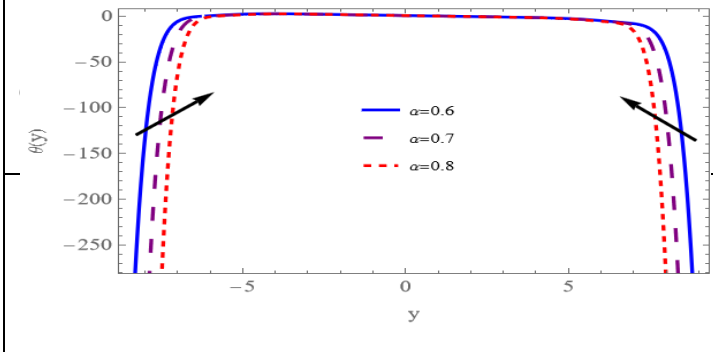


Figure 27: Variation of temperature θ with y for different value of (ϕ) when $Ha = 2$,

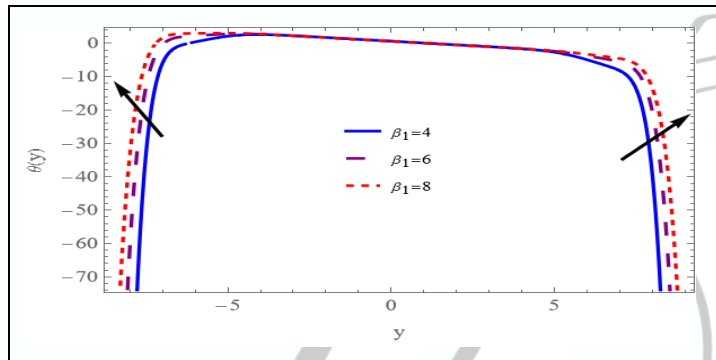
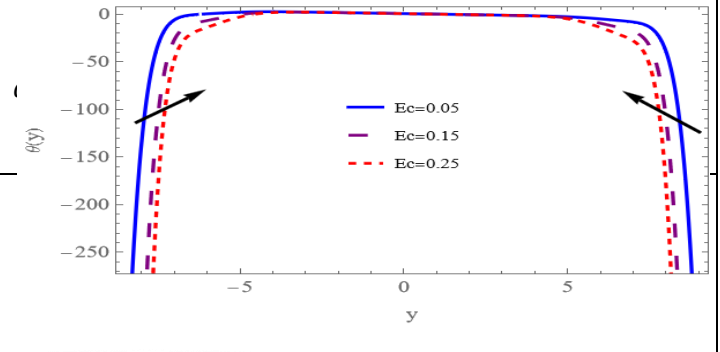


Figure34: Variation of temperature θ with y for different value of (β_1) when $Ha = 2$,

$\beta = 0.1, Da = 10, \rho = 0.1, d = 0.5, \Omega = 0.5,$
 $\mu = 3, w = 0.3, \phi = 1.3, \alpha = 0.2, b = 0.2,$
 $d_1 = 0.5, F0 = 0.5, F1 = 0, A = 0.1, \beta_1 = 4,$
 $Ec = 0.05, Pr = 0.05, \alpha = 0.6, Re = 2,$
 $Fr = 1, \alpha^* = 1.5$



Figure 28 :Variation of temperature θ with y for different value of (α) when $Ha = 2$,
 $\beta = 0.1, Da = 10, \rho = 0.1, d = 0.5, \Omega = 0.5,$
 $\mu = 3, w = 0.3, \phi = 1.3, a = 0.2, b = 0.2,$
 $d_1 = 0.5, F_0 = 0.5, F_1 = 0, A = 0.1, \beta_1 = 4,$
 $Ec = 0.05, Pr = 0.05, \alpha = 0.6, Re = 2,$
 $Fr = 1, \alpha^* = 1.5$

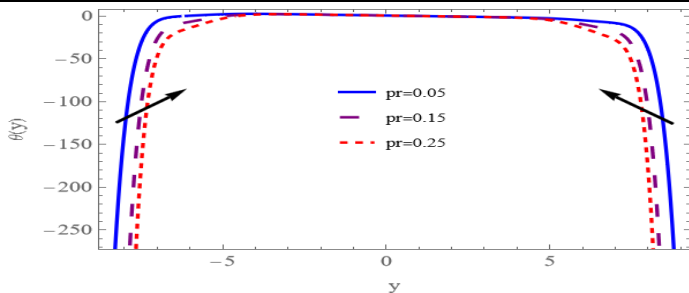


Figure ٢9:Variation of temperature θ with y for different value of (Ec) when $Ha = 2$,
 $\beta = 0.1, Da = 10, \rho = 0.1, d = 0.5, \Omega = 0.5,$
 $\mu = 3, w = 0.3, \phi = 1.3, a = 0.2, b = 0.2,$
 $d_1 = 0.5, F_0 = 0.5, F_1 = 0, A = 0.1, \beta_1 = 4,$
 $Ec = 0.05, Pr = 0.05, \alpha = 0.6, Re = 2,$
 $Fr = 1, \alpha^* = 1.5$

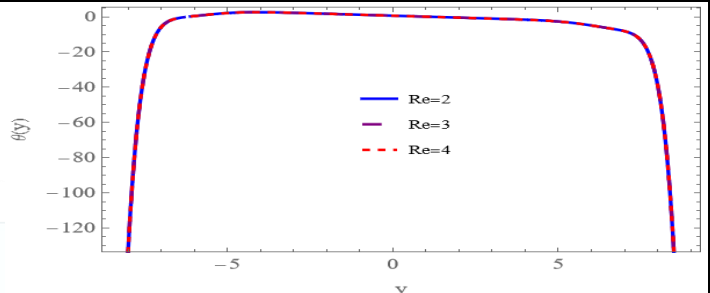


Figure 30:Variation of temperature θ with y for different value of (Pr) when $Ha = 2$,
 $\beta = 0.1, Da = 10, \rho = 0.1, d = 0.5, \Omega = 0.5,$
 $\mu = 3, w = 0.3, \phi = 1.3, a = 0.2, b = 0.2,$
 $d_1 = 0.5, F_0 = 0.5, F_1 = 0, A = 0.1, \beta_1 = 4,$
 $Ec = 0.05, Pr = 0.05, \alpha = 0.6, Re = 2,$
 $Fr = 1, \alpha^* = 1.5$

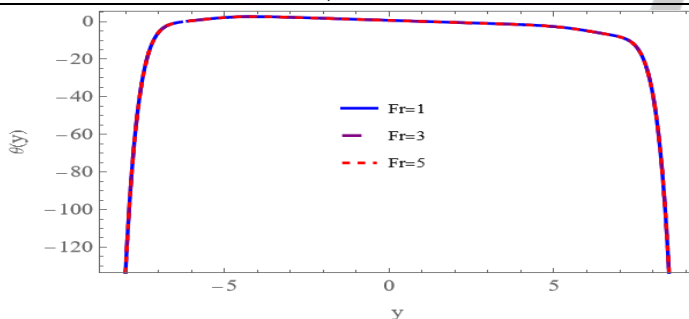


Figure ٣1: Variation of temperature θ with y for different value of (Re) when $Ha = 2$,
 $\beta = 0.1, Da = 10, \rho = 0.1, d = 0.5, \Omega = 0.5,$
 $\mu = 3, w = 0.3, \phi = 1.3, a = 0.2, b = 0.2,$
 $d_1 = 0.5, F_0 = 0.5, F_1 = 0, A = 0.1, \beta_1 = 4,$
 $Ec = 0.05, Pr = 0.05, \alpha = 0.6, Re = 2,$
 $Fr = 1, \alpha^* = 1.5$

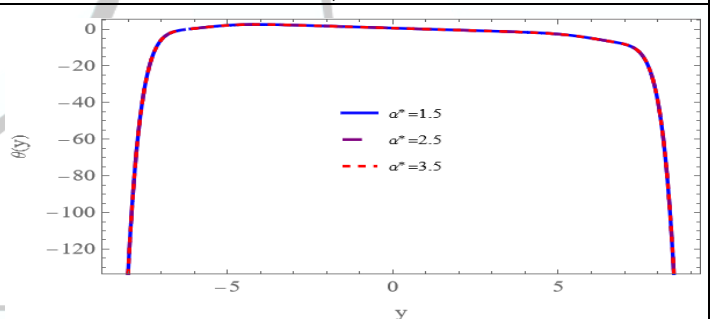


Figure 32:Variation of temperature θ with y for different value of (Fr) when $Ha = 2$,
 $\beta = 0.1, Da = 10, \rho = 0.1, d = 0.5, \Omega = 0.5,$
 $\mu = 3, w = 0.3, \phi = 1.3, a = 0.2, b = 0.2,$
 $d_1 = 0.5, F_0 = 0.5, F_1 = 0, A = 0.1, \beta_1 = 4,$
 $Ec = 0.05, Pr = 0.05, \alpha = 0.6, Re = 2,$
 $Fr = 1, \alpha^* = 1.5$

Figure 33:Variation of temperature θ with y for different value of (α^*) when $Ha = 2$,
 $\beta = 0.1, Da = 10, \rho = 0.1, d = 0.5, \Omega = 0.5,$
 $\mu = 3, w = 0.3, \phi = 1.3, a = 0.2, b = 0.2,$
 $d_1 = 0.5, F_0 = 0.5, F_1 = 0, A = 0.1, \beta_1 = 4,$
 $Ec = 0.05, Pr = 0.05, \alpha = 0.6, Re = 2,$
 $Fr = 1, \alpha^* = 1.5$



Figure34:Variation of temperature θ with y
for different value of (β_1) when $Ha = 2$,
 $\beta = 0.1, Da = 10, \rho = 0.1, d = 0.5, \Omega = 0.5$,
 $\mu = 3, w = 0.3, \phi = 1.3, a = 0.2, b = 0.2$,
 $d_1 = 0.5, F_0 = 0.5, F_1 = 0, A = 0.1, \beta_1 = 4$,
 $Ec = 0.05, Pr = 0.05, \alpha = 0.6, Re = 2$,
 $Fr = 1, \alpha^* = 1.5$

7. Conclusions

This study examines how coupling stress, slip condition, and rotation affect the peristaltic movement of a Powell-Eyring fluid through a porous medium that is vulnerable to inclined MHD and heat transfer.. The asymmetric channel is formed by selecting peristaltic waves with varying amplitudes and phases on the non-uniform walls and a low Reynolds number. The formulas for the axial velocity, pressure gradient, and temperature distribution are produced. Multiple graphs are utilized for parameter analysis:

I) When the values of Hartman number (Ha), the inclination of magnetic field (β), slip condition (β_1) increase, the axial velocity is rising close to the channel wall's margin, while the axial velocity decreases near the channel wall when the values of the rotation (Ω), the values of porous medium parameter (w), the amplitude ratio (ϕ), and couple stress parameter (α) increase and alsoThe axial velocity does not change as the increase of the values of Darcy number (Da). however all the above parameters does not effect on the axial velocity in the channel's central region.

II)

s the values of the Hartman number (Ha) and the porous medium parameter (w) increase, the curve of the pressure gradient decrease, the opposite occurs when the values of in the inclination of magnetic field (β), width of the channel (d), the rotation (Ω), couple stress parameter (α), and slip condition (β_1) increase, but that the pressure gradient does not change as values increase the Darcy number (Da), the Froude number (Fr), the Reynolds number (Re), and the inclination angle of the channel to the horizontal axis (α^*), the Reynolds number (Re), and the Froude number (Fr), and for



approximately $-4.2 < x < -1.2$ the axial velocity increases as the amplitude ratio increases (ϕ), but for approximately $x > -1.2$ and $x < -4.2$, the axial pressure gradient decreases.

III) As the of the Hartman number (Ha), the porous medium parameter (w), the amplitude ratio (ϕ), couple stress parameter (α), the Eckert number (Ec), and the Prandtl number (Pr) increases, the temperature field decreases in the vicinity of the channel's wall but no change in the channel's central region, while the increases in the values of the inclination of magnetic field (β) and the slip condition (β_1) there is no effect on the temperature field in the channel's central region, the temperature field increases in the vicinity of the channel's wall and furthermore increasing values of the Darcy number (Da), the rotation (Ω), the Reynolds number (Re), the Froude number (Fr), and the inclination angle of the channel to the horizontal axis (α^*) have no effect on the temperature field.

8. References

1. Abdulhussein, H., & Abdulhadi, A. M. (2022). Impact of Couple Stress and Rotation on Peristaltic Transport of a Powell-Eyring Fluid in an Inclined Asymmetric Channel with Hall and Joule Heating. *Journal of Basic Sciences*, 8(13).<http://bsj.uowasit.edu.iq>
2. Ahmed, T. S. (2018). Effect of Inclined Magnetic Field on Peristaltic Flow of Carreau Fluid through Porous Medium in an Inclined Tapered Asymmetric Channel. *Al-Mustansiriyah Journal of Science*, 29(3), 94–105.
3. Al-Khafajy, D. G. S. (2021). Influence of Varying Temperature and Concentration on Magnetohydrodynamics Peristaltic Transport for Jeffrey Fluid with a Nanoparticles Phenomenon through a Rectangular Porous Duct. *Baghdad Science Journal*, 18(2).
4. Ali, H. A. (2022). Impact of Varying Viscosity with Hall Current on Peristaltic Flow of Viscoelastic Fluid Through Porous Medium in Irregular Microchannel. *Iraqi Journal of Science*, 1265–1276.
5. Ali, H. A., & Abdulhadi, A. M. (2018). Analysis of Heat Transfer on Peristaltic Transport of Powell- Eyring Fluid in an Inclined Tapered Symmetric Channel with Hall and Ohm's Heating Influences. *Journal of Al-Qadisiyah for Computer Science and Mathematics*, 10(2), 26–41.
<https://doi.org/10.29304/jqcm.2018.10.2.364>
6. Aziz, A., Jamshed, W., Aziz, T., Bahaidarah, H. M. S., & Ur Rehman, K. (2021).



Entropy analysis of Powell–Eyring hybrid nanofluid including effect of linear thermal radiation and viscous dissipation. *Journal of Thermal Analysis and Calorimetry*, 143(2), 1331–1343. <https://doi.org/10.1007/s10973-020-10210-2>

7.Eldabe, N. T., Kamel, K. A., Ramadan, S. F., & Saad, R. A. (2020). Peristaltic motion of Eyring–Powell nano fluid with couple stresses and heat and mass transfer through a porous media under the effect of magnetic field inside asymmetric vertical channel. *Journal of Advanced Research in Fluid Mechanics and Thermal Sciences*, 68(2), 58–71.

8.Gamachu, D., & Ibrahim, W. (2023). Entropy production on couple-stress hybrid nanofluid flow in a rocket engine nozzle with non-Fourier’s and non-Fick’s law. *Ain Shams Engineering Journal*, 14(1), 101818.

9.Hage, A. K., & Hummady, L. Z. (2022). Influence of inclined magnetic field and heat transfer on peristaltic transfer Powell-Eyring fluid in asymmetric channel and porous medium. *International Journal of Nonlinear Analysis and Applications*.

10.Hayat, T., Aslam, N., Rafiq, M., & Alsaadi, F. E. (2017). Hall and Joule heating effects on peristaltic flow of Powell–Eyring liquid in an inclined symmetric channel. In *Results in Physics* (Vol. 7, pp. 518–528). <https://doi.org/10.1016/j.rinp.2017.01.008>

11.Hina, S., Mustafa, M., Hayat, T., & Alsaedi, A. (2016). Peristaltic flow of Powell–Eyring fluid in curved channel with heat transfer: A useful application in biomedicine. *Comput. Methods Programs Biomed.*, 135, 89–100.

12.Hummady, L. Z. (2022). Effect of Couple Stress on Peristaltic Transport of Powell–Eyring Fluid Peristaltic flow in Inclined Asymmetric Channel with Porous Medium. *Wasit Journal of Computer and Mathematics Sciences*, 1(2), 106–118.

13.Hussain, Q., Alvi, N., Latif, T., & Asghar, S. (2019). Radiative heat transfer in Powell–Eyring nanofluid with peristalsis. *International Journal of Thermophysics*, 40(5), 1–20.

14.Jasim, A. M. (2022). Study of the Impact of Unsteady Squeezing Magnetohydrodynamics Copper-Water with Injection-Suction on Nanofluid Flow Between Two Parallel Plates in Porous Medium. *Iraqi Journal of Science*, 3909–3924.

15.Kareem, R. S., & Abdulhadi, A. M. (2020). Impacts of Heat and Mass Transfer on Magneto Hydrodynamic Peristaltic Flow Having Temperature-dependent Properties in an Inclined Channel Through Porous Media. *Iraqi Journal of Science*, 854–869.

16.Khudair, W. S., & Dwail, H. H. (2021). Studying the Magnetohydrodynamics for Williamson Fluid with Varying Temperature and Concentration in an Inclined Channel with Variable Viscosity. *Baghdad Science Journal*, 18(3), 531.

17.Latham, T. W. (1966). *Fluid motion in peristaltic pumps*, M S. Thesis, MIT, Cambridge, MA. Retrieved from <https://dspace.mit.edu/handle/1721.1/17282>

18.Mohaisen, H. N., & Abedulhadi, A. M. (2022). Effects of the Rotation on the Mixed Convection Heat Transfer Analysis for the Peristaltic Transport of Viscoplastic Fluid in Asymmetric Channel. *Iraqi Journal of Science*, 1240–1257.



- 19.Noreen, S., Kausar, T., Tripathi, D., Ain, Q. U., & Lu, D. C. (2020). Heat transfer analysis on creeping flow Carreau fluid driven by peristaltic pumping in an inclined asymmetric channel. *Thermal Science and Engineering Progress*, 17, 100486.
- 20.Prasad, K. V., Choudhari, R., Vaidya, H., Bhat, A., & Animasaun, I. L. (2023). Analysis of couple stress nanofluid flow under convective condition in the temperature-dependent fluid properties and Lorentz forces. *Heat Transfer*, 52(1), 216–235.
- 21.Salman, M. R., & Abdulhadi, A. M. (2018). Influence of heat and mass transfer on inclined (MHD) peristaltic of pseudoplastic nanofluid through the porous medium with couple stress in an inclined asymmetric channel. *Journal of Physics: Conference Series*, 1032(1), 12043.
- 22.Satya Narayana, P. V, Tarakaramu, N., Moliya Akshit, S., & Ghori, J. P. (2017). MHD flow and heat transfer of an Eyring-Powell fluid over a linear stretching sheet with viscous dissipation-A numerical study. *Front. Heat Mass Transf*, 9(9).

JOBS



مجلة العلوم الأساسية
Journal of Basic Science



Print -ISSN 2306-5249

Online-ISSN 2791-3279

العدد السابع عشر

٢٠٢٣م / ١٤٤٤هـ



مجلة العلوم الأساسية
للعلوم التربوية والنفسية وطرائق التدريس للعلوم الأساسية